

Effect of a supercritical fluid on the characteristics of sorption processes

A. B. Rabinovich and Yu. K. Tovbin*

L. Ya. Karpov Physicochemical Research Institute
10 ul. Vorontsovo pole, 105064 Moscow, Russian Federation.
Fax: +7 (495) 975 2450. E-mail: tovbin@cc.nifhi.ac.ru

The effect of an inert supercritical (SC) component of a gas mixture on the equilibrium adsorption conditions was investigated theoretically. The adsorption isotherms were calculated within the framework of the lattice-gas model taking into account lateral interactions of the nearest neighbors in the quasichemical approximation. The physical adsorption and chemisorption isotherms were calculated at specified chemical potentials of the main and supercritical components and at specified mole fractions of the supercritical component. The binary phase diagrams SC component—atoms of the solid characterizing the solubility conditions of SC molecules in the solids are considered.

Key words: adsorption isotherms, physical adsorption, chemisorption, phase diagram, supercritical fluids.

The pressure increase in the gas phase as a result of surface processes (adsorption, catalytic, membrane, and some other processes) influences both the rates of elementary steps involving the gas components of the reaction system and the conditions of equilibrium of the components.^{1,2} Therefore, variation of the pressure in the gas is one of the ways for controlling the processes that occur on the surface.

Depending on the composition of the gas mixture, two cases can be distinguished. In one case, the gas mixture consists of readily adsorbed molecules that participate in the surface processes. A pressure increase in the system directly increases the concentration of adsorbed species (reactants). A classical example of such system is ammonia synthesis,³ which takes place at a pressure of several tens of atmospheres. In the other case, the gas mixture contains a plenty of molecules that are weakly adsorbed or not adsorbed at all. A pressure increase results in larger surface coverage by not only the main reactants, which are well adsorbed, but also by poorly adsorbed molecules. If the amount of poorly adsorbed molecules in the gas phase markedly exceeds the amount of the main reactants, their coverages would be commensurable. This type comprises many polymeric systems involving supercritical carbon dioxide (SC-CO₂), which is a solvent and a plasticizer for a number of polymers.⁴ It differs from traditional solvents by low cost, environmental safety, non-volatility, and ease of removal from the polymer after the process. The interest in the use of carbon dioxide is also related to the possibility of changing the morphological and functional properties of polymers upon their storage in SC-CO₂ and the ability of carbon dioxide to extract low-molecular-weight

compounds, residual solvents, and the monomers from polymers,⁵ which is a way for obtaining materials with a specified porous structure.

In this study, we analyze the effect of the supercritical fluid (SCF), first of all its concentration, on the characteristics of adsorption processes. For this purpose, the adsorption isotherms of one and two main components (components A and B) of a gas mixture in the presence of inert SCF (component C) were considered and the phase diagrams of the binary systems characterizing the conditions of mixing of SCF molecules with atoms of a solid (solubility) were constructed.

Calculation methods

Model. This study was performed within the framework of the condensed phase theory on the basis of the lattice-gas model.^{6,7} In this model, the system volume V is split into cells or species with the volume $v_0 = \lambda^3$ (λ is the lattice constant) corresponding to the size of a molecule; this precludes double occupation of a cell (adsorption site) by different molecules. Hence, the system volume is $V = Nv_0$, where N is the number of cells in the system. Each site of the lattice system with z neighboring sites can be occupied by a molecule of sort i (i is the number of system components) or a vacancy. Thus, the number of different occupation states of any system site (s) is equal to the number of components plus a vacancy.

Usually, the concentration of molecules is taken to be equal of the number of molecules per unit volume, $C_i = N_i/V$. In the lattice-gas model, the concentration of a fluid component is described by the surface coverage by species, $\theta_i = N_i/N$, which is the ratio of the number of species of the component i in volume $V(N_i)$ to the number of cells in the same

volume (N). Thus, $\theta_i = C_i v_0$. Complete coverage of the system is defined as

$$\theta = \sum_{i=1}^{s-1} \theta_i.$$

The partial pressures of the mixture components will be designated by p_i ($1 \leq i \leq s-1$). The equations that describe the adsorption of the mixture on a uniform surface or in the bulk of a solid at a specified temperature T , in the quasichemical approximation for interaction between the species can be represented as follows:

$$a_i p_i = \Lambda_i \left(\frac{\theta_i}{\theta_s} \right)^{g(T)}, \quad 1 \leq i \leq s-1 \quad (1)$$

where $a_i = \exp(\beta Q_i)$ are the Henry constants; Q_i is a bonding energy of species i to the surface; $\beta = (kT)^{-1}$; $g(T)$ is a calibrating function⁸ used, in the general case, to increase the accuracy of calculation in the vicinity of the critical temperature; in this work, $g(T) \equiv 1$.

The function Λ_i takes into account the interactions between z nearest molecules and is determined by the following relations:

$$\Lambda_i = (S_i)^z, \quad S_i = 1 + \sum_{j=1}^{s-1} x_{ij} t_{ij}, \quad x_{ij} = \exp(-\beta \epsilon_{ij}) - 1, \quad (2)$$

where $t_{ij} = \theta_{ij}/\theta_i$ are the transitional probabilities that species j is located near species i ; ϵ_{ij} is the interaction parameter of neighboring species i and j . In the case of the equilibrium state, pair correlation functions θ_{ij} are the solutions of the following algebraic system of equations:

$$\theta_{ij} \theta_{ss} = \theta_{is} \theta_{sj} \exp(-\beta \epsilon_{ij}), \quad \sum_{j=1}^s \theta_{ij} = \theta_i, \quad \sum_{i=1}^s \theta_i = 1. \quad (3)$$

Solution of system of equations (1)–(3) by the Newton iteration method at a specified set of $\{\theta_i\}$ or $\{P_i\}$ values allows one to calculate all the equilibrium characteristics of the system.

Lateral interactions put in order the spatial distribution of molecules. The pair distribution functions θ_{ij} characterize the probabilities that species of sorts i and j occur in neighboring cells. It follows from Eq. (3) that if $\epsilon_{ij} > 0$, species i and j are attracted and $\theta_{ij} > \theta_i \theta_j$. If $\epsilon_{ij} < 0$, species i and j are repulsed and $\theta_{ij} < \theta_i \theta_j$.

In the absence of interactions between the molecules, the equations are transformed to well-known equations for ideal reaction systems for which $\theta_{ij} = \theta_i \theta_j$ (see Refs 9–11). Equations (1)–(3) are simplified to be transformed to adsorption equations for an ideal mixture $a_i p_i = \theta_i/\theta_s$, $\sum_{i=1}^s \theta_i = 1$. In particular, for one-component adsorption ($s = 2$), they are transformed to the Langmuir equation describing the adsorption of molecules on isolated sites.

Equations (1) and (2) refer to the case where all components of the mixture have commensurable geometric sizes. Equations taking into account the difference between real molecules and spherical molecules and/or the orientation of molecules were derived.¹² The CO_2 molecule is not strictly spherical, its aspect ratio being ~ 1.38 . Since the density of SCF is intermediate between the vapor and liquid densities, for dense vapors, the aspect ratio of carbon dioxide molecule in the supercritical state can be taken to be unity.

Calculation conditions. Usually, the temperature of SC processes exceeds the critical temperature T_c by a factor of not more than three; therefore, the dimensionless value $\tau = T/T_c$ will be used as the temperature.

The interaction energy of system components ϵ_{ij} will also be specified in the dimensionless form by normalizing ϵ_{ij} to $\epsilon_0 = \epsilon_{CC}$ and taking that $\gamma_i = \epsilon_{ii}/\epsilon_0$. We also assume that $\epsilon_{ij} = \epsilon_0(\gamma_i \gamma_j)^{1/2}$ (see Ref. 13). The lateral interaction parameters (γ) are defined as positive values for physical adsorption and are negative for chemisorption.

The interaction energy of the adsorbate with the surface is characterized by the value $Q_i = b_i |\epsilon_{ii}|$, where coefficient b_i defines the factor by which this energy exceeds the interaction energy of the component i molecules with their neighbors. The interactions with b_i values of about 1.5–2.5 are considered weak, being typical of interactions of adsorbed molecules with polymeric matrices. If $b_i > 4$, these interactions are classified as strong. For an inert SCF, most important is the case where $b_C \ll 1$, where C is the SC component of a many-component system. In our calculations, we assumed that $b_C = 0.1$.

Results and Discussion

Physical adsorption. Figures 1 and 2 present the results of calculation of physical adsorption isotherms of component **A** in the presence of SCF at a constant partial pressure of the main component **A** on weakly ($b_A = 2$) and strongly ($b_A = 9.2$) adsorbing surfaces. The P_A values corresponding to three different surface coverages by component **A** ($\theta_A = 0.05, 0.5$, and 0.85) were used in the calculations. Each curve in Fig. 1 describes the effect of the partial pressure of component **C** on the surface coverage by component **C** at a constant pressure of component **A**. The curves in Fig. 2 show how the increase in the partial pressure of component **C** affects the surface coverage by component **A** at an invariable pressure of component **A**.

As can be seen from Fig. 1, an increase in the partial pressure of SCF entails an increase in the surface coverage by component **C**. The rate of growth of the density θ_C almost does not depend on whether the surface contains weak or strong adsorption sites.

As the SCF pressure increases, the surface coverage by component **A** decreases (see Fig. 2); thus, as the SCF pressure increases, component **A** is being replaced from the adsorbent surface. A comparison of Figs 2, *a* and 2, *b* leads to the conclusion that on the strongly adsorbing surface, component **A** is displaced from adsorption sites at higher SCF pressures than on a weakly adsorbing surface. For the strongly adsorbing surface, the replacement proceeds more slowly and over a broader range of pressures of component **C** than for the weakly adsorbing surface.

In order to follow the effect of temperature on the pattern of physical adsorption of a mixture of components **A** and **C**, construct the adsorption isotherms in the $(\theta - \ln P)$ coordinates, where $\theta = \theta_A + \theta_C$ is the total coverage, $P = P_A + P_C$ is the total isothermal pressure. The adsorption isotherms of component **A** in the presence of inert SC

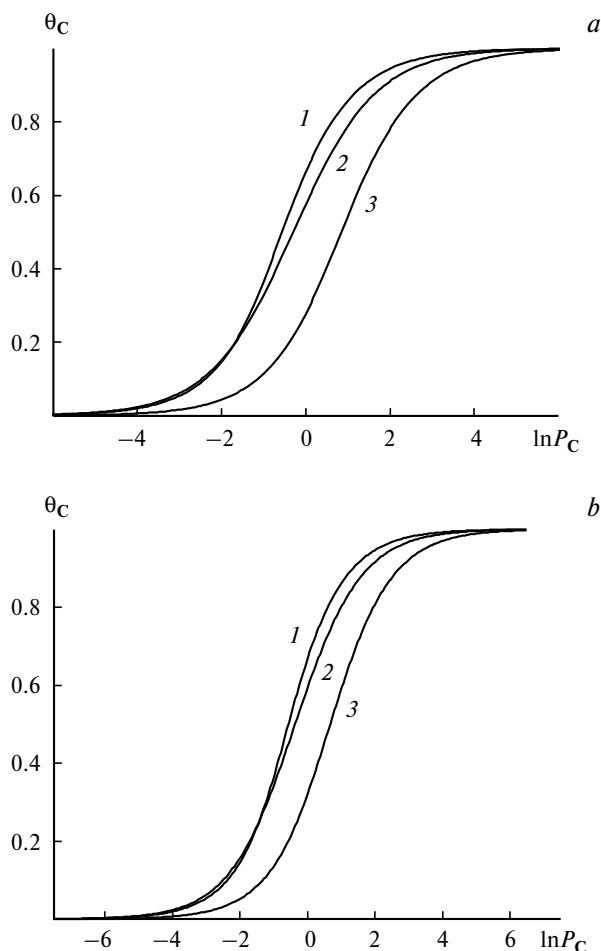


Fig. 1. Adsorption isotherm of the SC component **C** mixed with component **A** in the $\ln P_C$ – θ_C coordinates on the surfaces with $b_A = 2$ (a) and 9.2 (b) at constant partial pressures of component **A** (P_A) corresponding to surface coverages $\theta_A = 0.05$ (1), 0.5 (2), and 0.85 (3).

component **C** for the cases where the surface concentrations of the main component θ_A are 0.01 and 0.1 are shown in Fig. 3. All adsorption isotherms start at the points corresponding to θ_A values. The curves for $\theta_A = 0.1$ are shifted to the right along the θ axis and down along the $\ln P$ axis with respect to the curves constructed for $\theta_A = 0.01$; as the density θ increases, these curves approach each other.

The adsorption isotherms were constructed for three temperatures, $\tau = 0.625$, 1.25, and 4 ($\tau = T/T_C$). At supercritical temperatures $\tau > 1$, adsorption isotherms monotonically increase, being situated in the region of thermodynamic stability of equilibrium isotherms. Below the critical temperature, $\tau = 0.625$, the adsorption isotherms have a local minimum at high coverages, which corresponds to the thermodynamic instability region called the van der Waals loop.

The calculation of the adsorption isotherms of two components (**A** and **B**) in the presence of an inert SCF

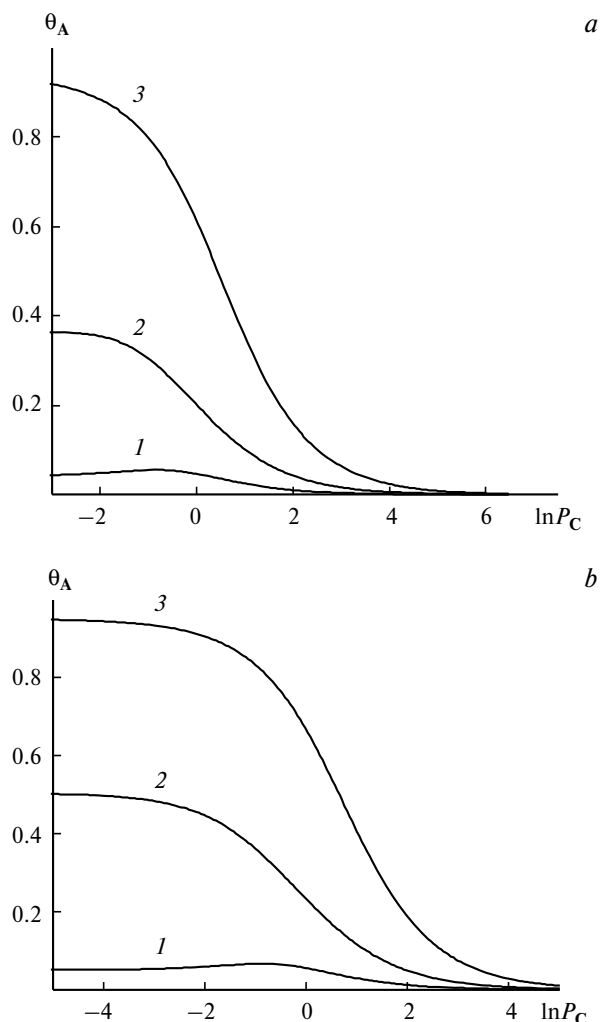


Fig. 2. Adsorption isotherm of the main component **A** in the presence of SCF in the $\ln P_C$ – θ_A coordinates on the surfaces with $b_A = 2$ (a) and 9.2 (b) at constant partial pressures of component **A** (P_A) corresponding to surface coverages $\theta_A = 0.05$ (1), 0.5 (2), and 0.85 (3).

allows one to elucidate the effect of lateral interaction parameters on the character of adsorption. The calculations were carried out at two values of the lateral interaction parameter, $\gamma_B = 4.0$ and 9.4, two temperatures, $\tau = 1.15$ and 2.5, and two concentrations of the main component, $\theta_A = 0.01$ and 0.1 (Fig. 4). The adsorption isotherms shown in Fig. 4 are similar to those of the two-component system considered above, because they were constructed with the assumption that the concentrations θ_A and θ_B are constant and $\theta_A = \theta_B$.

As can be seen in Fig. 4, an increase in the amounts of the main components **A** and **B** changes the course of P/θ dependence: all adsorption isotherms start at the points corresponding to $\theta_A + \theta_B$ values. In addition, the higher the temperature $\tau > 1$, the faster the increase in $\ln P$ as a function of θ . A comparison of Figs 4, a and 4, b shows

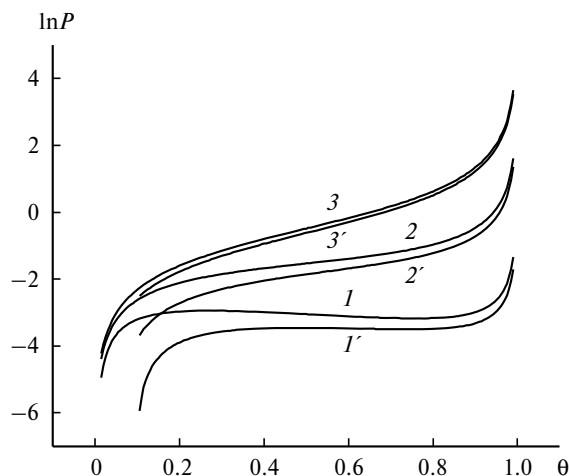


Fig. 3. Adsorption isotherms of a binary system in the θ – $\ln P$ coordinates for surface coverages by main component $\theta_A = 0.01$ (1, 2, 3), and 0.1 (1', 2', 3') and temperatures corresponding to $\tau = 0.625$ (1, 1'), 1.15 (2, 2'), and 4 (3, 3').

that at low θ_A values, a change in the attraction force between the molecules of the main components **A** and **B** has little influence on the isotherm shape. At higher θ_A values, an increase in the attraction force between the molecules of the main components leads to upward shift of the adsorption isotherm along the $\ln P$ axis, *i.e.*, the curve corresponding to greater lateral interaction parameter γ_B is located above the curve for lower γ_B value. The greatest difference between the curves is attained when the initial values $\theta = \theta_A + \theta_B$. As the density θ increases, the adsorption isotherms approach each other.

Chemisorption. Examples of chemisorption isotherms of component **A** in the presence of SCF at $\tau = 3.3$ are shown in Fig. 5. As the SCF pressure increases, the main component **A** is being replaced at any of initial θ_A : 0.05, 0.5, or 0.85. The course of the chemisorption isotherms qualitatively coincides with the course of physical adsorption isotherms, although the ranges of pressure of the main component **A** differ by approximately six orders of magnitude for chemisorption and physical adsorption (see Fig. 2). However, comparison of Figures 2 and 5 shows that at the same SCF pressure, the surface coverage by the main component θ_A is much higher for chemisorption than for physical adsorption due to higher energy of the species surface bond.

A comparison of the chemisorption isotherms shown in Figs 5, *a* and *b* demonstrates that an increase in the energy of interaction between chemisorbed species and the surface changes little the pattern of replacement of these species from the surface by the inert component **C**. This is attributable to the fact that the energy of interaction of chemisorbed species with the surface sharply increases, and for large surface bond energies Q_i the effect of SCF decreases.

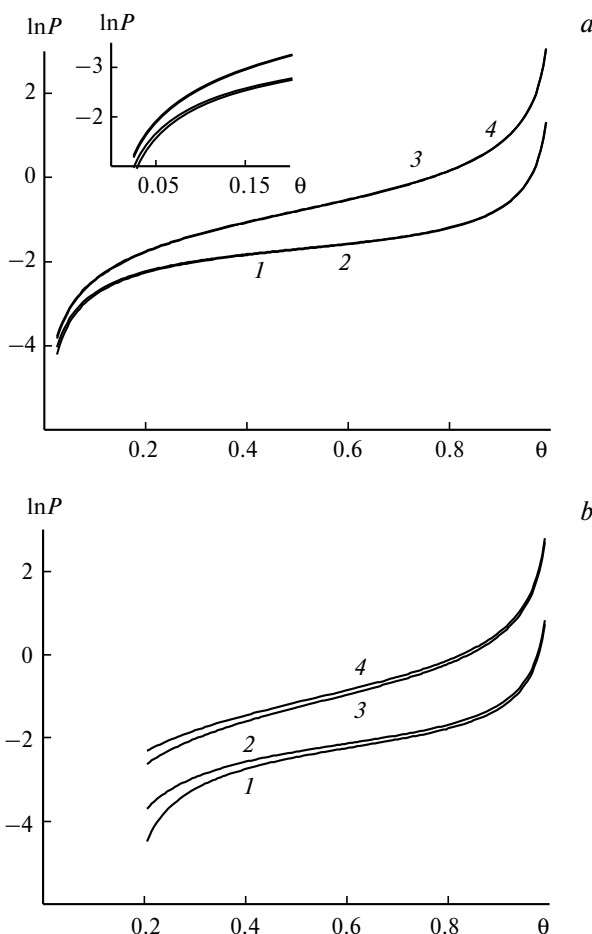


Fig. 4. Adsorption isotherms of a ternary system in the θ – $\ln P$ coordinates for surface coverages by components **A** and **B** $\theta_A = \theta_B = 0.01$ (*a*) and 0.1 (*b*) at temperatures corresponding to $\tau = 1.15$ (1, 2) and 2.5 (3, 4) and lateral interaction parameters $\gamma_B = 4.0$ (1, 3) and 9.2 (2, 4). The inset shows the initial sections of adsorption isotherms 1–4 at $\theta_A = \theta_B = 0.01$.

All the adsorption and chemisorption isotherms considered above, except for curves 1 and 1' in Fig. 3, refer to postcritical temperatures $\tau > 1$. At these temperatures, adsorption isotherms increase monotonically with a pressure increase in the gas phase. However, the properties of the system below the critical temperature, at $\tau \leq 1$, which characterize the mixing conditions of SCF molecules and atoms of the solid, are equally important.

Separation curves. At any $\tau < 1$, the adsorption isotherm has a thermodynamic instability region called the van der Waals loop. Using the Maxwell rule, it is possible to find the values of surface coverage for coexisting liquid $\theta^L(\tau)$ and vapor $\theta^V(\tau)$ phases. By expressing the found θ values in the θ – τ coordinates, we obtain two curves that meet at $\tau = 1$. Connecting these two curves in the θ – τ coordinates gives a dome-shaped curve with the top at $\tau = 1$. This dome-shaped curve is called coexistence curve or separation phase diagram.

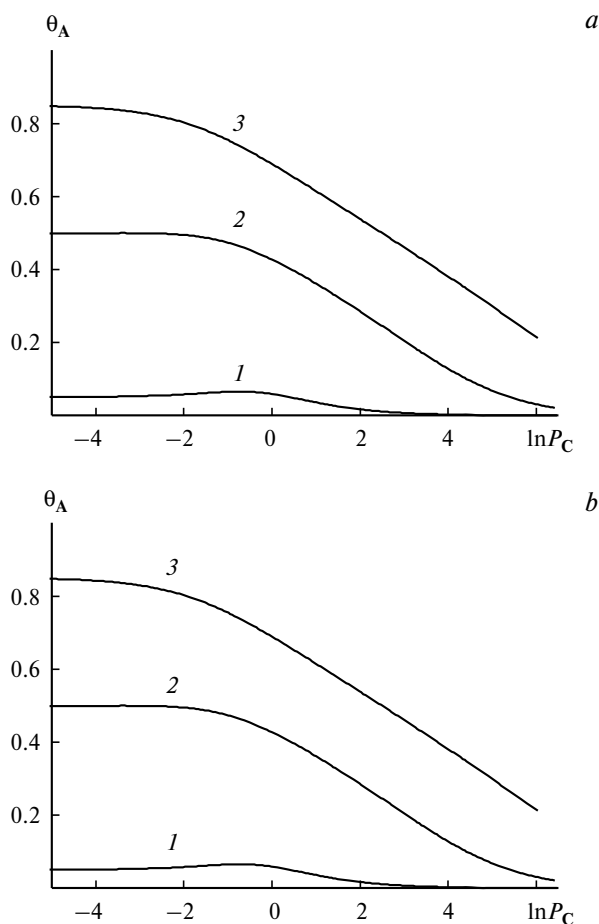


Fig. 5. Chemisorption isotherms of component A in the presence of SCF in the $\ln P_C$ – θ_A coordinates for surface coverages $\theta_A = 0.05$ (1), 0.5 (2), and 0.85 (3). Lateral interaction parameter $\gamma_A = 3.15$.

The phase diagrams of separation of atoms of the main component and the SC component for $\gamma_A = 2$, *i.e.*, under the assumption that the lateral interaction parameters are similar, are shown in Fig. 6. The dashed curve refers to pure A. The addition of component C changes the adsorption isotherms, and, hence, the separation diagram. Component C can be added in two ways: 1) with a specified constant percentage or fraction of component C (continuous lines) or 2) with a specified concentration θ_C (dashed lines) (see Fig. 6). Since at a constant concentration θ_C (the second case of addition of component C), the adsorption isotherms start at $\theta = \theta_C$, the initial points of the state diagram also occur at $\theta = \theta_C$. An increase in both the amount and the fraction of SC component C results in a decrease in the critical temperature and shifts the dome top to lower densities. This behavior indicates that upon the action of any inert SCF at sufficiently high pressure on component A, the bonds between the atoms of the main component are weakened.

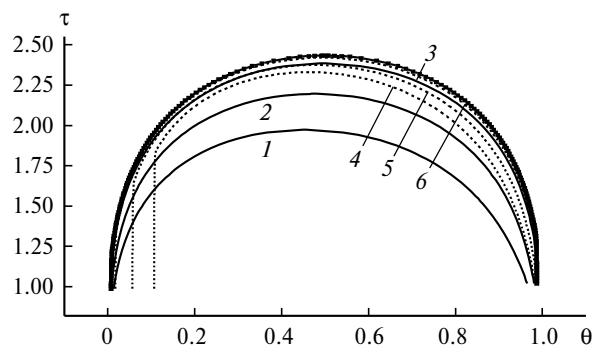


Fig. 6. Separation curves for the molecules of component A in the θ – τ coordinates for mixtures containing 10 (1), 5 (2), and 3% (3) of SC component C and for mixtures with surface coverages $\theta_C = 0.1$ (4), 0.05 (5), and 0.01 (6). The separation curve for pure component A is shown by dashed line. Lateral interaction parameter $\gamma_A = 2$.

A more complicated case of phase diagram where the interaction between the molecules of main component A exceeds the interaction between the SCF molecules approximately 10-fold is presented in Fig. 7. Here four rather than two coexisting phases are possible, which gives rise to a two-top phase diagram where the second dome can separate from the main dome and transform to a closed curve.

Figure 7 shows the state diagrams for $\gamma_A = 6.3$ and different fractions of the inert SC component. The numbers at the curves correspond to percentages of component C in a mixture of species A and C. The dashed line corresponds to pure component A, and the dome close to curve 10 corresponds to pure component C. As the fraction of component C in the mixture increases, the

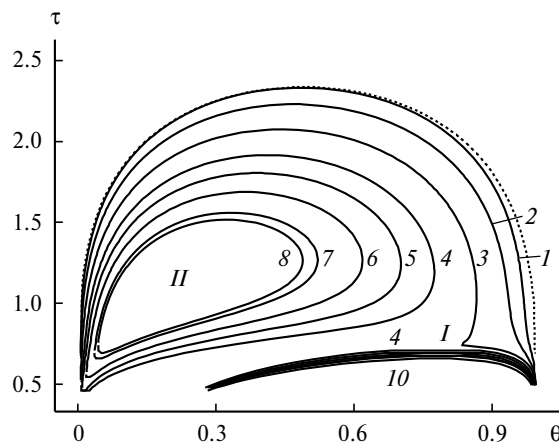


Fig. 7. Separation curves for the molecules of component A in the presence of SCF in the θ – τ coordinates. The numbers at the curves correspond to percentages of component C; the separation curve of pure component A is shown by dashed line. Lateral interaction parameter $\gamma_A = 6.3$. The Figure also shows a kink in curve 1 and the region of disappearance of the curves of the upper part of diagram II.

shape of the separation curve becomes more and more complicated.

The effect of component **C** starts to be manifested at $C_C \geq 1\%$. The dome shifts to the left, to lower density values, and at high θ values, it is pressed against curve *10*. It can be seen especially clearly for $C_C \approx 3\%$: the corresponding diagram has kink *I*. The shape of the curve to the left of the kink is affected by component **A**, while the shape of the curve to the right of the kink at high density θ values is dictated by the effect of component **C**. When the fraction of component **C** is about 4%, the left and right parts of the diagram are separated. The diagram is split into two parts, the upper and lower ones. The upper part of the diagram formed under the influence of component **A** becomes a separate closed curve. The lower part, which reflects the effect of component **C**, becomes the main dome. This can be seen especially clearly for $C_C \approx 4\%$. On further increase in the fraction of component **C** in the mixture ($C_C > 4\%$), the effect of component **A** is mitigated and the upper closed curve narrows down (closed curves 5–8). At $C_C \approx 10\%$, the upper part of the diagram disappears in the region *II* and only the main dome remains. Meanwhile, the lower parts of curves 5–8, which are located between curves 4 and 10, gradually shift down approaching the main dome (see Fig. 7, curve 10).

It can be seen from Fig. 7 that SCF can lead to pronounced changes in the phase diagrams if the bond energy between the molecules of component **A** is high as compared with the bond energy between the SCF molecules. The dome for the main component **A** is highly deformed, the separation curves acquire a very complex pattern and depend substantially on the content of component **C**. The most important feature of the separation curves shown in this diagram is that they become much lower at high density values θ . This is indicative of considerable weakening of bonding of the main component to the surface as the main component is being replaced by component **C**. This effect can be observed for $\gamma_A < 10$, which is typical of polymeric matrices. If the parameter γ_A is high ($\gamma_A \approx 10^2$), which is typical of oxides or metals, the presence of SCF does not play a significant role.

Thus, in this work we studied the effect of an inert supercritical component of a gas mixture on the equilibrium conditions of the adsorption of molecules. The adsorption isotherms were calculated in terms of the lattice-gas model taking into account the lateral interactions of the close neighbors in the quasichemical approximation. The concentration dependences for fixed chemical potentials of the main and supercritical components and for

fixed molar fraction of the supercritical component in the physical adsorption and chemisorption processes are considered. The binary phase diagrams SCF—atoms of the solid, which characterize the solubility conditions for SCF molecules in solids, are analyzed. The results of calculations attest to pronounced effect of SCF on the equilibrium characteristics of the adsorption and absorption of gas mixtures. For quantitative description of particular SC systems, it is necessary to take into account the real size of the main components and SCF, including the orientation effects of large molecules.¹²

This work was supported by the Russian Foundation for Basic Research (Project No. 09-03-12144 ofi_m).

References

1. Savage, S. Gopalan, T. I. Mizan, C. J. Martino, E. E. Brock, *AIChE J.*, 1995, **41**, 1723.
2. D. Yu. Zalepugin, N. A. Til'kunova, I. V. Chernyshova, V. S. Polyakov, *Sverkhkriticheskie flyuidy: teoriya i praktika* [*Supercritical Fluids: Theory and Practice*], 2006, **1**, 27 (in Russian).
3. M. I. Temkin, *Zh. Fiz. Khim.*, 1950, **24**, 1312 [*Russ. J. Phys. Chem. (Engl. Transl.)*, 1950, **24**].
4. A. I. Cooper, *J. Mater. Chem.*, 2000, **10**, 207.
5. M. A. McHugh, V. J. Krukons, *Supercritical Fluid Extraction: Principles and Practice*, Butterworth Publ., Stoneham, 1994, 507 pp.
6. T. L. Hill, *Statistical Mechanics. Principles and Selected Applications*, McGraw-Hill, New York, 1956, 448 pp.
7. Yu. K. Tovbin, *Teoriya fiziko-khimicheskikh protsesov na granitse gaz—tverdoe telo* [*Theory of Physicochemical Processes on the Gas—Solid Interface*], Nauka, Moscow, 1990, 288 pp. (in Russian).
8. Yu. K. Tovbin, A. B. Rabinovich, *Langmuir*, 2004, **20**, 6041.
9. S. L. Kiperman, *Osnovy khimicheskoi kinetiki v geterogennom katalize* [*Foundations of Chemical Kinetics in Heterogeneous Catalysis*], Khimiya, Moscow, 1979, 350 pp. (in Russian).
10. E. N. Eremin, *Osnovy khimicheskoi kinetiki* [*Foundations of Chemical Kinetics*], Vysshaya shkola, Moscow, 1976, 374 pp. (in Russian).
11. S. W. Benson, *The Foundations of Chemical Kinetics*, McGraw-Hill, New York, 1960, 703 pp.
12. Yu. K. Tovbin, *Izv. Akad. Nauk, Ser. Khim.*, 1997, 458 [*Russ. Chem. Bull. (Engl. Transl.)*, 1997, **46**, 437].
13. J. O. Hirschfelder, Ch. F. Curtiss, R. B. Bird, *Molecular Theory of Gases and Liquids*, John Wiley and Sons, New York, 1954, 1219 pp.

Received February 28, 2010;
in revised form July 5, 2010